Z-RAFT Star Polymerizations of Acrylates: Star Coupling via Intermolecular Chain Transfer to Polymer

Daniel Boschmann and Philipp Vana*

Institut für Physikalische Chemie, Georg-August-Universität Göttingen, Tammannstr. 6, D-37077 Göttingen, Germany

Received December 1, 2006; Revised Manuscript Received January 25, 2007

ABSTRACT: Six-arm star polymers of methyl acrylate (MA), butyl acrylate (BA), and dodecyl acrylate (DA) were generated in bulk at 60 °C via reversible addition−fragmentation chain transfer (RAFT) polymerization. A hexafunctional trithiocarbonate was employed as mediating compound, in which the active RAFT-agent moieties are interlinked to the central core molecule via the stabilizing Z-group. Well-defined star polymers with predictable number-average molecular weights of more than 1×10^6 g·mol^{-1} were obtained by this Z-RAFT star polymerization of acrylates. Narrow and monomodal molecular weight distributions were found up to intermediate monomer conversions. At higher monomer conversions, an unexpected high molecular weight component occurred with increasing extent when going from MA over BA to DA polymerization. This high molecular weight material was assigned to a star−star couple containing two living cores, which formation is not in accordance to the basic Z-RAFT star polymerization mechanism, but most likely arises from an *inter*molecular chain transfer to polymer reaction. The amount of star−star couples, which is an indication for the extent of long-chain branching, was quantified as a function of the monomer conversion and subsequently modeled via kinetic simulations. By this approach, the rate coefficient of *inter*molecular transfer to polymer at 60 °C was estimated to be $k_{tr}^{P,inter} = 0.33$ L·mol^{-1}·s^{-1} in BA polymerization and $k_{tr}^{P,inter} = 7.1$ L·mol^{-1}·s^{-1} in DA polymerization. The living process was found to be very effective up to high monomer conversions, indicating that steric congestion next to the star polymer core, where the actual RAFT process takes place, is not significantly hampering the Z-RAFT star polymerization of acrylates.

Introduction

Star polymers, i.e., macromolecules with one distinct central branching point and several polymeric arms, are attracting attention because of their interesting characteristics: they show a decreased zero-shear viscosity and a decreased steady-state compliance in comparison to linear polymer with the same molecular weight,[1,2] which makes them attractive as rheology modifiers in oils and lubricants for automotives.[3,4] They are used in adhesives because of their high resistance to low-stress peel while maintaining moderate adhesion,[5] they can influence crystallization characteristics,[6] and they have a pronounced impact on the self-assembly of polymers leading to nanostructured polymeric materials.[7,8] Due to their well-defined macromolecular topology, star polymers have also attracted interest in life sciences, where they find applications in the field of drug release[9] and serve as unimolecular polymeric micelles.[10,11] In the past, star polymers were mostly generated via anionic polymerization, which limited the monomer choice and caused star polymers to be relatively expensive materials due to their time-consuming production. With the advent of controlled/living radical polymerization (C/LRP), star polymers from of a multitude of monomers—including functional and water-soluble monomers—became accessible with relative ease. This sparked intensive research into these complex macromolecular architectures and into associated material properties.[12]

Preparation of star polymers can be grouped into two approaches: (i) the arm-first and (ii) the core-first method. In the arm-first approach, the linear arms of the star polymer are first synthesized, followed by coupling to the core. Because of steric effects, however, complete functionalization of the core is often not quantitative using this approach. The core-first method, on the other side, allows better control over the star polymer architecture. This strategy proceeds via the synthesis of a multifunctional agent, which constitutes the core, followed by the extension of arms from this agent by monomer addition. This approach guarantees a predefined number of arms and enables facile manipulation of the polymeric end groups at the tip of the arms. By adding a defined star-shaped mediating agent to a core-first C/LRP, star polymer is created in a controlled fashion with predetermined topology.

The applicability of C/LRP toward the formation of star polymers via the core-first approach has been demonstrated in several studies,[13−18] with the vast majority of the work performed via atom transfer radical polymerization (ATRP)[19] and nitroxide-mediated polymerization (NMP).[20] Comparably few studies report the application of reversible addition−fragmentation chain transfer (RAFT)[21] polymerization for star polymer formation.[22−29] RAFT, however, is especially promising for star polymerizations, due to its specific mechanism that allows for two alternative approaches toward star polymer synthesis (see Scheme 1). This provides an increased flexibility for star polymer design within the concept of the core-first method, i.e., the mediating agent may be linked to the core either via the leaving R-group or via the stabilizing Z-group.

The R-RAFT star approach (see Scheme 1) is in essence equivalent to the star polymerization mechanism operative in other C/LRP techniques and may lead to star−star coupling via termination of two star polymers carrying a radical center.[22] Such coupling is also frequently observed in core-first ATRP and NMP star polymerizations,[30,31] which generally restricts the star polymerization to the low monomer conversion regime and impedes the formation of high molecular weight material. Moreover, the R-RAFT star polymerization mechanism leads to the loss of RAFT functionality at the star-shaped RAFT agent,

* Corresponding author. E-mail address: pvana@uni-goettingen.de.

10.1021/ma0627626 CCC: $37.00
Published on Web 03/14/2007

Scheme 1. Approaches to Star Polymers via RAFT Polymerization within the Concept of the Core-First Method

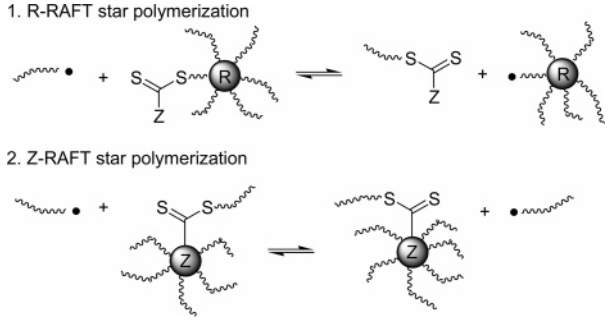

and the formation of linear living chains in solution (see Scheme 1). This complex situation leads to multimodal and broad chain-length distributions of star polymer with drastically decreased structural homogeneity.[22,25,32]

In contrast, the dithioester RAFT functionality is not departing from the star molecule when using the Z-RAFT approach (see Scheme 1), which prevents the formation of linear living polymer. Furthermore, star−star coupling by the conventional radical−radical termination reaction is excluded, since the propagating radical is in principle never located at the star molecule.[23,29] Termination events—unavoidable in any RAFT polymerization—will take place between two free "arm"-macroradicals yielding linear dead polymer. These mechanistic features are unique to the Z-RAFT star polymerization and guarantee a highly improved homogeneity of the generated star polymer.[23] High monomer conversions, i.e., high molecular weights of uniform star polymer are thus accessible. The fact that the controlling thiocarbonylthio moieties sit close to the core was, however, speculated to disturb the effectiveness of the controlling RAFT process with increasing arm length due to shielding effects, and deviations of experimental molecular weights from theoretical predictions have been attributed to steric congestion.[29,33] Interestingly, such deviation has been observed in the Z-RAFT star polymerizations of styrene[26] and vinyl acetate,[23] but no deviation could be identified in the Z-RAFT star polymerization of butyl acrylate.[33]

Although the mechanistic requirements for uniform star polymer formation are fulfilled by Z-RAFT star polymerization, side reactions of an unidentified nature may disturb the homogeneity of the final polymeric product, limiting its applicability. During our work on Z-RAFT star polymerizations, which we are utilizing for the formation of building blocks for molecular containers and supramolecular structures, we observed unexpected side reactions in the case of acrylates being the monomers: at higher monomer conversions, a high molecular weight component was observed in the molecular weight distributions of the generated star polymer, which is not in agreement with the basic reaction scheme given in Scheme 1. Similar observations have been made in linear RAFT polymerizations of acrylates using various RAFT agents,[34] as well as in linear ATRP of methyl acrylate,[35] suggesting that this phenomenon is general to radical acrylate polymerization. It was recently hypothesized by Postma et al.[36] that the high molecular weight shoulder occurring in linear RAFT polymerization of acrylates arises from copolymerization of polyacrylate macromonomers that are formed during the polymerization by a β-scission reaction after intramolecular backbiting.

It is the objective of the present work to characterize Z-RAFT star polymerizations of acrylates and to elucidate the reaction mechanism that induces the formation of high molecular weight material. It will be probed, whether the mechanism proposed by Postma et al.[36] can be responsible for the occurrence of high molecular weight components in Z-RAFT star polymerizations of acrylates. Star polymerizations are especially beneficial for this purpose, as the scenario of having individual living polymeric species, i.e., the arms, being interlinked to an assembled overall structure, i.e., the star, allows to separate the coupled living material (i.e., potential star−star couples) from the dead polymer, which occurs at lower molecular weight than the star polymer, because it originates from the termination of two growing arm macroradicals. This feature provides mechanistic and structural insights that cannot be obtained from linear RAFT polymerization. Consequently, the molecular weight distributions of polymer from methyl acrylate, butyl acrylate, and dodecyl acrylate Z-RAFT star polymerizations mediated by a hexafunctional trithiocarbonate are studied in detail up to high monomer conversions. A mechanism for the unexpected formation of high molecular weight components in Z-RAFT star polymerizations of acrylates is proposed and is subsequently employed for estimating rate coefficients of intermolecular transfer to polymer via computer modeling.

Materials and Methods

Chemicals. Dipentaerythritol hexakis(3-mercaptopropionate) (**1**) was obtained from Wako Chemicals and used without further purification. The initiator 2,2′-azobis(isobutyronitrile) (AIBN, Merck) was recrystallized from diisopropyl ether before usage; the purity was more than 98% as verified by ^{1}H NMR analysis. Methyl acrylate (MA, ≥99.0%, Fluka), butyl acrylate (BA, ≥99.0%, Fluka), and dodecyl acrylate (DA, ≥90.0%, where the remaining part is tetradecyl acrylate, Fluka) were purified by passing through a column filled with inhibitor remover for hydroquinone and methyl hydroquinone (Aldrich). Column-chromatographic purification of the RAFT agent was performed using silica gel (Merck, Kieselgel 60) and technical grade *n*-pentane and ethyl acetate. Tetrahydrofuran used as the eluent in size-exclusion chromatography (THF, Carl Roth, Rotipuran, stabilized with 2,6-di-*tert*-butyl-4-methylphenol) was used as received. All other chemicals were purchased from Aldrich and used without further purification.

Dipentaerythritol Hexakis(3-*S*-(methyl-2-propanoatotrithiocarbonyl)propanoate) (2). The synthetic pathway to **2** is outlined in Scheme 2 and is based on a protocol reported by Mayadunne et al.[25] A solution of triethylamine (6.07 g, 60 mmol, in 15 mL of $CHCl_3$) was added dropwise to a stirred solution of **1** (3.92 g, 5 mmol) and carbon disulfide (4.57 g, 60 mmol) in $CHCl_3$ (20 mL) at room temperature. After 1 h a solution of methyl 2-bromopropanoate (5.85 g, 35 mmol, in 15 mL of $CHCl_3$) was added dropwise to the reaction mixture. After 2 h, the mixture was poured into a cold solution of 10% aqueous HCl and extracted three times with ethyl acetate to afford a thick yellow oil. The crude product was purified via column chromatography on silica gel using a solvent gradient going from pentane:ethyl acetate = 3:1 (R_f = 0.01) to pure ethyl acetate (R_f = 0.94). The product **2** was obtained as a yellow oil (7.29 g, 83%).

^{1}H NMR ($CDCl_3$) δ (ppm): 1.54 (d, J = 7.2 Hz, 18H, CH_3), 2.72 (t, J = 6.8 Hz, 12H, CH_2), 3.54 (t, J = 6.8 Hz, 12H, CH_2), 3.68 (s, 18H, CH_3), 4.05 (s, 16H, CH_2), 4.75 (q, J = 7.2 Hz, 6H, CH).

^{13}C NMR ($CDCl_3$) δ (ppm): 16.73 (CH_3), 31.11 ($C(CH_2OR)_4$), 31.24 (CH_2), 32.74 (CH_2), 42.88 (CH_2), 47.92 (CH), 52.86 (OCH_3), 62.54 (CH_2), 171.60 (C═O), 171.94 (C═O), 221.49 (C═S).

Anal. Calcd.: C, 39.66; H, 4.71; S, 32.86. Found: C, 39.05; H, 4.65; S, 31.92.

Electrospray ionization mass spectrometry: m/z 1772.05 (theoretical: m/z 1772.04, M + NH_4^+).

Polymerizations. Monomers were degassed via three freeze−pump−thaw cycles, transferred along with RAFT agent and initiator into an argon-filled glovebox (oxygen content below 1.5 ppm) where stock solutions of 10 mL monomer, initiator (AIBN), and

Scheme 2. Synthesis Strategy of Star-Shaped RAFT Agent 2

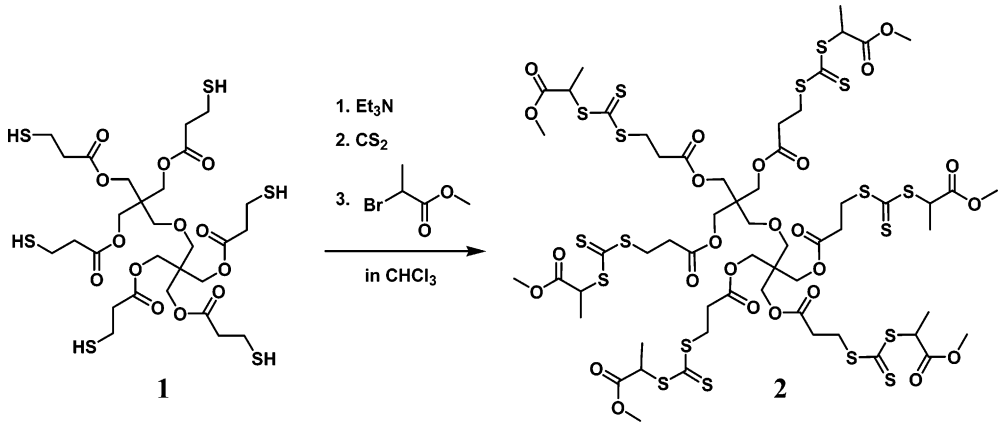

hexafunctional RAFT agent **2** were prepared. A few drops of toluene were added in the case of DA polymerization to guarantee the dissolving of the RAFT agent. Ten samples of each stock solution were filled into individual glass vials and sealed with Teflon/rubber septa. The vials were subsequently inserted into a block heater thermostated at 60 ± 0.1 °C. The samples were removed after preset time intervals and the reactions were stopped by cooling the solutions in an ice bath. The reaction times were up to 10 h for MA, up to 5 h for BA, and up to 1.7 h for DA. Monomer to polymer conversions were determined gravimetrically for the MA and BA systems and via calibrated areas under the refractive index detector signal of the SEC in the case of DA.

Cleavage of Star Polymer.[37] Around 20 mg of polymer and 20 mg of AIBN were dissolved in 5 mL of toluene. The sample was sealed with a Teflon/rubber septum, deoxygenated by nitrogen purging for approximately 10 min, and then kept for 24 h at 60°. After filtering, the solution the filtrate was evaporated to remove the volatiles.

Instrumentation. Molecular weight distributions were determined by size-exclusion chromatography (SEC) using a JASCO AS-2055-plus autosampler, a Waters 515 HPLC pump, three PSS−SDV columns with nominal 5 μm particle size and pore sizes of 10^5, 10^3, and 10^2 Å, a Waters 2410 refractive index detector, a Viskotek VE3210 UV/vis-detector, and THF at 35 °C as the eluent at a flow rate of 1.0 mL·min^{-1}. The SEC setup was calibrated with polystyrene standards of narrow polydispersity (M_p = 410 to 2000000 g·mol^{-1}) from Polymer Standards Service. Mark−Houwink parameters for linear polystyrene ($K = 1.41 \times 10^{-2}$ mL·g^{-1} and $a = 0.700$),[38] linear poly(MA) ($K = 1.68 \times 10^{-2}$ mL·g^{-1}, $a = 0.696$),[39] linear poly(BA) ($K = 1.22 \times 10^{-2}$ mL·g^{-1}, $a = 0.700$),[40] and linear poly(DA) ($K = 2.92 \cdot 10^{-2}$ mL·g^{-1}, $a = 0.585$)[41] were employed to recalculate the molecular weight distributions according to the principle of universal calibration. The inter-detector delay between RI− and UV-detection was considered for comparing the respective chain-length distributions. Mass spectrometry was performed on a Finnigan LCQ ion trap electrospray ionization mass spectrometer (ESI-MS) equipped with an atmospheric pressure ionization source and operated in the nebulizer-assisted electrospray mode. For further details regarding the ESI-MS setup, see ref 42. NMR spectroscopy was performed using a Varian Mercury 200. Elemental analysis was carried out on a Heraeus CHN−O-Rapid Analyzer and on a METROHM 662 photometer equipped with a 636 Tiroprocessor.

Computational Methods. The kinetic modeling was performed by using the program package PREDICI, version 6.4.4., including the parameter estimation module. Multiple peak fitting was performed using ORIGIN, version 7.0.

Results and Discussion

As star-shaped Z-RAFT agent, we employed the hexafunctional trithiocarbonate **2** (see Scheme 2), which is similar to the star-shaped RAFT agent introduced by Mayadunne et al.,[25] but carries a methyl acrylate moiety instead of benzyl as leaving group. The reason for this choice of leaving group is 2-fold: First, the acrylate-type leaving group radical guarantees good reinitiation characteristics for the studied acrylate polymerizations, and, second, this type of leaving group gives rise to star polymer end groups, which do not exhibit any UV-absorbance above 300 nm (see below). The star-shaped Z-RAFT agent **2** was then employed as mediating agent in AIBN-initiated methyl acrylate (MA), butyl acrylate (BA), and dodecyl acrylate (DA) bulk polymerization at 60 °C, and well controlled characteristics, i.e., increasing molecular weight with progressive monomer conversion and polydispersities below 1.5 were identified in all systems. In MA star polymerization (see Figure 1), the experimental number-average molecular weights, $\bar{M}_n$, which were obtained via SEC that has been calibrated with linear polymer standards, were found to be below the theoretical molecular weights, $\bar{M}_n^{theo}$, at all employed RAFT agent concentrations, with the deviation becoming more pronounced at low concentration of **2**.

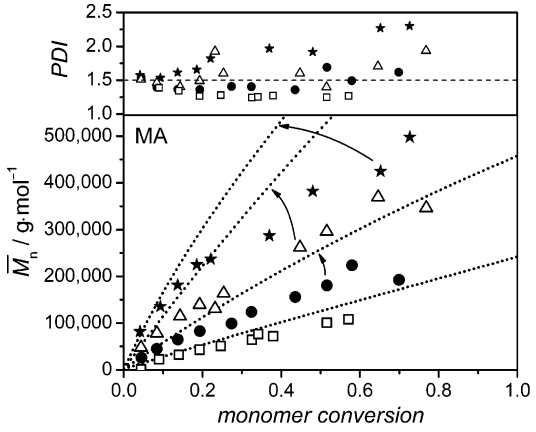

Figure 1. Number-average molecular weight, $\bar{M}_n$, and polydispersity index, PDI, in Z-RAFT star polymerizations of MA in bulk at 60 °C using AIBN as the initiator and **2** as star-shaped Z-RAFT agent. Key: (★) $c_2 = 0.46 \times 10^{-3}$ mol·L^{-1}, $c_{AIBN} = 1.71 \times 10^{-3}$ mol·L^{-1}; (△) $c_2 = 0.81 \times 10^{-3}$ mol·L^{-1}, $c_{AIBN} = 1.52 \times 10^{-3}$ mol·L^{-1}; (●) $c_2 = 1.53 \times 10^{-3}$ mol·L^{-1}, $c_{AIBN} = 1.83 \times 10^{-3}$ mol·L^{-1}; (□) $c_2 = 3.50 \times 10^{-3}$ mol·L^{-1}, $c_{AIBN} = 1.71 \times 10^{-3}$ mol·L^{-1}. The data was obtained via SEC that has been calibrated by linear polymer standards. The dotted lines indicate the theoretical molecular weights according to eq 1; the arrows identify to which theoretical molecular weight line the respective data set belongs.

The theoretical molecular weights, $\bar{M}_n^{theo}$, were calculated by eq 1:

$$\bar{M}_n^{theo} = \frac{X c_M{}^0 M_{monomer}}{c_{RAFT}{}^0 + c_I{}^0 \, df(1 - e^{-k_d t})} + M_{RAFT} \qquad (1)$$

with the fractional monomer conversion, X, the initial monomer concentration, $c_{M,}^0$ the initial RAFT agent concentration, c_{RAFT}^0, the initial radical initiator concentration, c_I^0, the molecular weights of monomer, $M_{monomer}$, and of RAFT agent, M_{RAFT}, with d being the number of chains that are generated in the termination process ($d \approx 1$ for acrylates),[43] with the initiator decomposition rate coefficient, k_d, and initiator efficiency, f ($k_d = 1.103 \times 10^{-5}$ s^{-1} [44] and $f = 0.7$ [45] was used for all studied systems). It should be noted that uncertainties in f, which might decrease when going from MA over BA to DA polymerization due to viscosity reasons,[46] have only a minor impact on $\bar{M}_n^{theo}$. The denominator of eq 1 represents the total concentration of polymer chains, which is steadily increasing with the reaction time t. Frequently, a simplified form of eq 1, in which a constant number of chains is assumed, is used to evaluate the molecular weight evolution in RAFT polymerization. This assumption generally holds in the case that the number of chains that are produced by the continuous initiation is small in comparison to the overall concentration of the employed RAFT agent, i.e., the concentration of living chains. In the present study, however, systems with very small concentrations of star-shaped RAFT agents were studied in order to arrive at star polymeric material of very high molecular weights. The amount of initiator-derived chains can therefore not be neglected in comparison to the number of living chains, which necessitated the use of eq 1.

The negative deviation of the experimental molecular weights from theoretically predicted values in the MA system (see Figure 1) can be explained by the reduced coil size of star polymers in solution in comparison to linear polymer of the same molecular weight.[47] As the molecular weights were evaluated via size-exclusion chromatography, which was calibrated with linear polymer samples and which separates polymer samples in accordance to their coil size, this behavior comes as no surprise and is providing independent evidence that star polymer has indeed be formed during the **2**-mediated MA polymerization. The average molecular weights and polydispersities reported in this study are consequently apparent values. The polydispersities of the generated star polymer was relatively low, as expected for an efficient C/LRP, and became higher with lower RAFT agent concentration (see Figure 1). PDI values below 1.5 could be observed up to monomer conversions of 60% when using Z-RAFT star agent concentrations exceeding 1.5 mmol·L^{-1}. A minimum PDI of 1.24 was observed with $c_2 = 3.50$ mmol·L^{-1}. The low RAFT agent concentrations were chosen to arrive at high molecular weights. It should, however, also be noted that the molar concentration of active trithiocarbonate-groups in the system is six times higher than the molar concentration of the star-shaped RAFT agent, since **2** constitutes a hexafunctional compound. The interlinking of individual living chains into one star-shaped molecule is an additional cause for the very high molecular weights that can be obtained when performing RAFT star polymerizations, e.g., about 400 000 g·mol^{-1} in MA polymerization after 50% of monomer conversion (see Figure 1). The scenario of having six individual RAFT polymers being bound together allows for accessing molecular weights that are roughly six times as high as commonly reached by classical linear RAFT polymerizations.

Whereas the **2**-mediated polymerization of MA is in first conclusion not exhibiting any unpredicted distinctive features, the Z-RAFT star polymerization of BA on the other hand shows

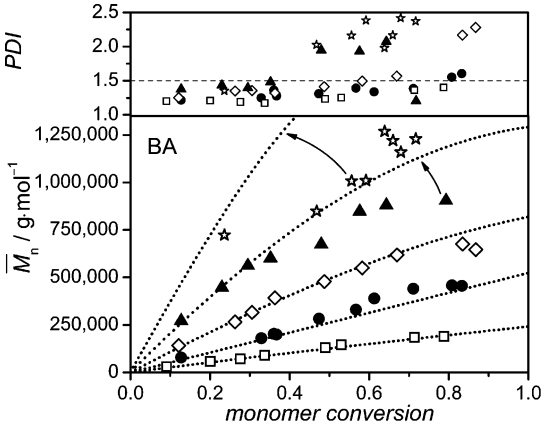

Figure 2. Number-average molecular weight, $\bar{M}_n$, and polydispersity index, PDI, in Z-RAFT star polymerizations of BA in bulk at 60 °C using AIBN as the initiator and **2** as star-shaped Z-RAFT agent. Key: (☆) $c_2 = 0.22 \times 10^{-3}$ mol·L^{-1}, $c_{AIBN} = 1.58 \times 10^{-3}$ mol·L^{-1}; (▲) $c_2 = 0.44 \times 10^{-3}$ mol·L^{-1}, $c_{AIBN} = 1.71 \times 10^{-3}$ mol·L^{-1}; (◇) $c_2 = 0.84 \times 10^{-3}$ mol·L^{-1}, $c_{AIBN} = 1.83 \times 10^{-3}$ mol·L^{-1}; (●) $c_2 = 1.60 \times 10^{-3}$ mol·L^{-1}, $c_{AIBN} = 1.89 \times 10^{-3}$ mol·L^{-1}; (□) $c_2 = 3.48 \times 10^{-3}$ mol·L^{-1}, $c_{AIBN} = 1.83 \times 10^{-3}$ mol·L^{-1}. The data was obtained via SEC that has been calibrated by linear polymer standards. The dotted lines indicate the theoretical molecular weights according to eq 1; the arrows identify to which theoretical molecular weight line the respective data set belongs.

an unexpectedly good match between experimental and theoretical molecular weights (see Figure 2). Similar to the MA system, a negative deviation of experimental data would have been anticipated, due to the smaller coil size of star polymers. Such deviation, however, can only be observed at RAFT agent concentrations below 0.5 mmol·L^{-1} and above 50% of monomer conversion. In the initial polymerization phase, polydispersities of the obtained star polymer are somewhat smaller than in the MA polymerization and show values well below 1.5, even at very low monomer conversion. This finding is indicative of a rapid initiation of the living process, i.e., a pre-equilibrium with a high probability for the fragmentation of the leaving group radical and/or its rapid reinitiation in BA polymerization. With 0.22 mmol·L^{-1} of **2**, star-shaped poly(BA) of molecular weights exceeding 1 million g·mol^{-1} is accessible, however, with associated PDI values of 2 and above. Star polymers with PDI values below 1.5 can be obtained up to $\bar{M}_n = 500\,000$ g·mol^{-1} (see Figure 2). A minimum PDI of 1.17 was observed at $\bar{M}_n = 90\,000$ g·mol^{-1} with $c_2 = 3.48$ mmol·L^{-1}.

Inspection of Figure 3, in which the molecular weight data of **2**-mediated DA polymerization is depicted, reveals that the experimental molecular weights in the case of DA polymerization even exceed the theoretical values significantly, which cannot be brought in agreement with the picture of coil sizes being smaller with star polymers. The molecular weight control in the DA system is slightly inferior in comparison to the MA and BA system as indicated by the observed PDI values: star polymer with PDI values below 1.5 can be obtained up to $\bar{M}_n = 300\,000$ g·mol^{-1} and a minimum PDI of 1.26 was observed at $\bar{M}_n = 80\,000$ g·mol^{-1} with $c_2 = 3.29$ mmol·L^{-1}. Again, star polymer of $\bar{M}_n = 500\,000$ g·mol^{-1} could be obtained after already 50% of monomer conversion. Polymerizations exceeding 60% of monomer conversion, however, showed pronounced gelation yielding insoluble material, which impeded polymer sampling.

Interestingly, in all studied systems no pronounced ceasing of chain growth was observed at high molecular weights, as has been observed with Z-RAFT star polymerization of styrene[29,33] and vinyl acetate,[23] and which has been attributed to

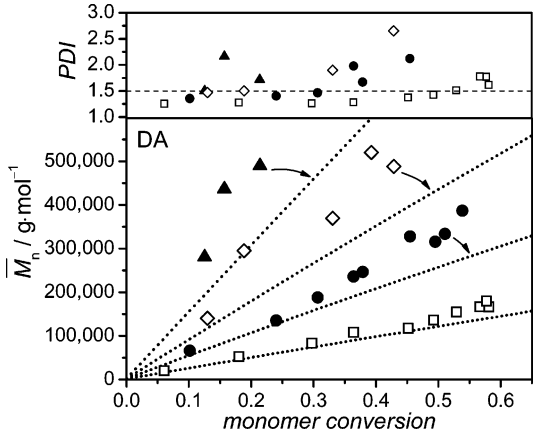

Figure 3. Number-average molecular weight, $\bar{M}_n$, and polydispersity index, PDI, in Z-RAFT star polymerizations of DA in bulk at 60 °C using AIBN as the initiator and **2** as star-shaped Z-RAFT agent. Key: (▲) $c_2 = 0.51 \times 10^{-3}$ mol·L^{-1}, $c_{AIBN} = 1.51 \times 10^{-3}$ mol·L^{-1}; (◇) $c_2 = 0.89 \times 10^{-3}$ mol·L^{-1}, $c_{AIBN} = 1.55 \times 10^{-3}$ mol·L^{-1}; (●) $c_2 = 1.52 \times 10^{-3}$ mol·L^{-1}, $c_{AIBN} = 1.55 \times 10^{-3}$ mol·L^{-1}; (□) $c_2 = 3.29 \times 10^{-3}$ mol·L^{-1} $c_{AIBN} = 1.77 \times 10^{-3}$ mol·L^{-1}. The data was obtained via SEC that has been calibrated by linear polymer standards. The dotted lines indicate the theoretical molecular weights according to eq 1; the arrows identify to which theoretical molecular weight line the respective data set belongs.

the increased steric hindrance occurring in systems mediated by Z-RAFT agents.[29] Even with DA that carries a sterically demanding ester moiety, molecular weight control is observed up to high molecular weights. It can hence be concluded that the key kinetic event in polyacrylate systems is fast enough to guarantee an effective RAFT equilibrium, even with the mediating groups located near the center of the growing star polymer (also see below). Steric hindrances in Z-RAFT star polymerization can thus not be regarded as a general issue, but may be specific to certain monomer systems or possibly have other causes. Theoretical investigations into the chain conformations occurring during Z-RAFT star polymerizations are currently underway.

The finding that the experimental molecular weights are first below the theoretical values, then match the predications and finally exceed the expected values when going from MA over BA to DA points toward a reason that is connected to some characteristic features of radical acrylate polymerization, rather than being related to the RAFT process itself. When inspecting the full molecular weight distributions of star polymer generated in **2**-mediated acrylate polymerization, an increasing amount of high molecular weight material can be observed with increasing monomer conversion. This effect is illustrated in Figure 4 on the example of **2**-mediated BA polymerization: (a) At low monomer conversions, uniform monomodal star polymer is generated, as expected from an ideal Z-RAFT star polymerization. (b) At higher monomer conversions, the chain length distribution becomes trimodal: terminated polymer originating from radical−radical termination between two growing arms (see Scheme 1) is occurring at molecular weights lower than that of the living main peak. It should be stressed that the terminated polymer in Z-RAFT star polymerization exhibits smaller molecular weights than the living star polymer. In the present case (Figure 4b), the terminated polymer is on average about three times smaller than the living material, in full accordance with termination via combination, which is considered the major pathway of termination in acrylate polymerization. In addition to the hump at low molecular weight, an unexpected high molecular weight shoulder occurs, which is in disagreement to the basic reaction scheme given in Scheme 1.

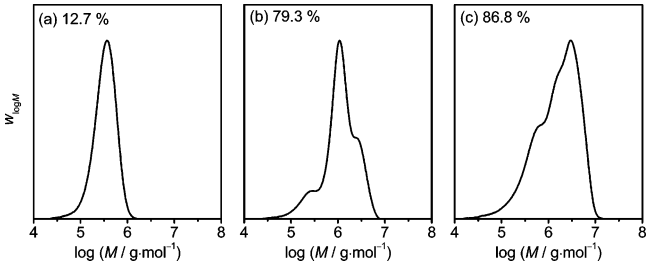

Figure 4. Normalized molecular weight distributions (SEC curves, i.e., weight distributions vs a logarithmic molecular weight axis) of polymer from a **2**-mediated ($c_2 = 0.44 \times 10^{-3}$ mol·L^{-1}) AIBN-initiated ($c_{AIBN} = 1.71 \times 10^{-3}$ mol·L^{-1}) Z-RAFT star polymerization of BA in bulk at 60 °C; samples are taken after (a) 12.7%, (b) 79.3%, and (c) 86.8% of monomer conversion.

Because of the fact that a Z-RAFT star polymerization system is studied, it can be excluded that this high molecular weight material originates from termination by the conventional star−star coupling mechanism observed when using the R-RAFT approach. The molecular weight of the high molecular weight shoulder is approximately double the value of the living main peak, e.g., the ratio between the peak molecular weight of the main peak (M_p = 1088000 g·mol^{-1}) and that of the high molecular weight peak (M_p = 2354000 g·mol^{-1}) depicted in Figure 4b, is 1 : 2.16. (c) With progressive monomer conversion both the terminated polymer peak and the high molecular weight peak are significantly increasing, eventually exceeding the size of the original main peak.

It is the progressive occurrence of this high molecular weight material that leads to experimental $\bar{M}_n$ values being higher than those expected on the basis of eq 1 with additional consideration of smaller coil size in the case of star polymers. Whereas in **2**-mediated MA polymerization hardly any high molecular weight material can be observed up to very high monomer conversions, the extent of high molecular weight material formation is increasing when going from BA to DA polymerization (see below).

In order to probe the nature of this high molecular weight material, a dual-detection approach after size-exclusion chromatography was performed, using sequential differential refractive index (RI) and UV-absorbance detection. The UV-detection was set to $\lambda = 310$ nm, where the trithiocarbonate moieties of the star-shaped RAFT agent exhibit a very strong absorption maximum,[48] whereas the polyacrylate backbone and the star polymer end groups originating from the reinitiating group (see above) are completely transparent. By such an approach, the core of the living Z-RAFT star polymer can be traced individually. First, the molecular weight distribution was evaluated via RI-detection, which is sensitive to the overall mass fraction of the polymer, thus giving a mass distribution vs a logarithmic molar mass axis, w_{logM}, as common in SEC chromatography. Second, the molecular weight distribution was evaluated via UV detection, which records the molar concentration of the trithiocarbonate-moieties, i.e., the cores of the living star polymer. Since each star polymer molecule is assumed to have one core, irrespective of the chain length of the attached arms, this detection mode yields a number distribution vs a logarithmic molar mass axis, x_{logM}. In the case, the assumption of one core per molecule holds, these two distributions may be transformed into each other via eq 2[49]

$$w_{\log M} = \frac{1}{\bar{M}_n} x_{\log M} M \qquad (2)$$

where $(\bar{M}_n)^{-1}$ constitutes the normalizing factor. Consequently,

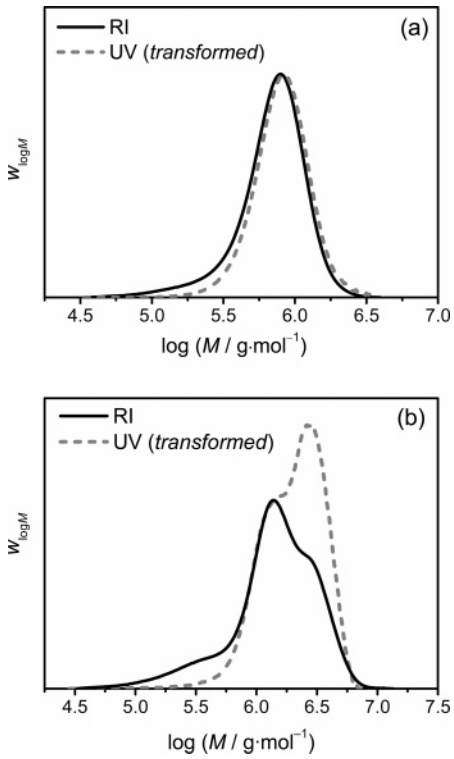

Figure 5. Normalized molecular weight distributions (SEC curves, i.e., weight distributions vs a logarithmic molecular weight axis, w_{logM}) evaluated both from RI-detection and UV-detection ($\lambda = 310$ nm) of polymer from a **2**-mediated ($c_2 = 0.44 \times 10^{-3}$ mol·L^{-1}) AIBN-initiated ($c_{AIBN} = 1.71 \times 10^{-3}$ mol·L^{-1}) Z-RAFT star polymerization of BA in bulk at 60 °C; samples are taken after (a) 29.5%, and (b) 64.3% of monomer conversion. The raw UV-signal has been transformed into the w_{logM} distribution according to eq 2.

the chain length distributions from UV-detection were transformed via eq 2 and, considering the inter-detector delay, compared to the chain length distributions from RI detection. Please note that the uncertainty in the molecular weights, which originates from the systematic deviation of apparent molar masses of star polymer from the true values (see above) will not affect the transformation in its essence, but the normalizing factor only. Inspection of Figure 5a shows an excellent agreement between these two distributions for star polymer obtained at relatively low monomer conversion. Small deviations at the low molecular weight slope of the peak originate from the fact that the conventionally terminated linear polymer does not carry any UV-absorbing trithiocarbonate-group and is therefore transparent in the UV-detection. The good agreement between RI and transposed UV chain-length distribution is in accordance with the expectation that the entire amount of living star polymer contains the same number of trithiocarbonate-type cores, presumably one. Inspection of Figure 5b, however, in which RI and transposed UV chain-length distribution of star polymer after relatively high monomer conversion is depicted, shows a significant deviation from the scenario expected for an ideal Z-RAFT star polymerization. Whereas the terminated polymer peak at the low molecular weight slope − as expected for linear terminated polyacrylate − is again not showing any UV-absorbance, the high molecular weight peak described above appears amplified in the UV chain-length distribution. Two important conclusions can be drawn from inspection of Figure 5b: (i) The high molecular weight material is living, because it contains active trithiocarbonate groups. (ii) The assumption of one core per polymer molecule—which was basis for the application of eq 2—does apparently not hold for this high

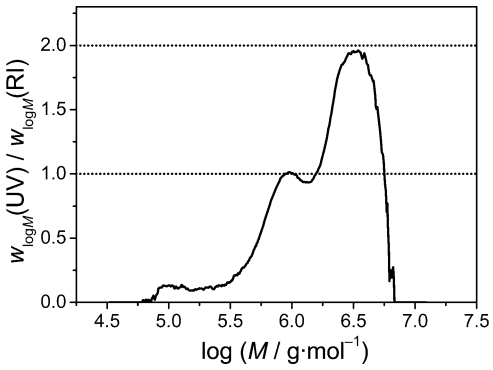

Figure 6. Ratio between molecular weight distributions from RI-detection and UV-detection ($\lambda = 310$ nm, transformed via eq 2), w_{logM}(UV)/w_{logM}(RI), of polymer from a **2**-mediated ($c_2 = 0.44 \times 10^{-3}$ mol·L^{-1}) AIBN-initiated ($c_{AIBN} = 1.71 \times 10^{-3}$ mol·L^{-1}) Z-RAFT star polymerization of BA in bulk at 60 °C after 64.3% of monomer conversion.

molecular weight material. The UV-signal intensity being higher than expected is thus indication of more absorbing groups per molecule in the high molecular weight material in comparison to the star polymer of the main peak.

The UV-absorbance is, according to Lambert−Beer's law, proportional to the number of absorbing moieties. The number of absorbing groups per polymer molecule can consequently be assessed by comparing the ratio of the chain-length distribution from UV-detection that has been transformed according to eq 2, w_{logM}(UV), with the chain-length distribution from RI-detection, w_{logM}(RI). Inspection of Figure 6—in which the ratio w_{logM}(UV)/w_{logM}(RI) has been normalized to unity at the molecular weight of the main peak where one core per star polymer is assumed—clearly indicates that the number of absorbing cores is approximately doubled with the high molecular weight material.

The finding that the molecular weight of the high molecular weight material is approximately double the value of that of the living star polymer and that this high molecular weight material exhibits exactly double the number of UV-absorbing core moieties is very strong evidence that a well-defined star−star coupling reaction occurs in Z-RAFT star polymerization of acrylates.

As already mentioned in the introduction, high molecular weight peaks have already been observed earlier in classical linear RAFT polymerizations of acrylates.[34] In linear RAFT polymerization, however, it is not trivial to separate polymer that was coupled by some unknown mechanism from the terminated polymer fraction, as these two species emerge at identical molecular weights. In an attempt to trace both end groups of linear poly(BA) from RAFT polymerization simultaneously by UV-absorption measurements, Postma et al.[36] arrived at the conclusion that the doubling of the molecular weight results from the copolymerization of macromonomers having similar chain lengths than the living polymer. These macromonomers were speculated to form via β-scission reaction of midchain radicals, which readily form in acrylate polymerization via backbiting reactions, i.e., via *intra*molecular transfer to polymer.[50] Although a small contribution of the reaction sequence suggested by Postma et al. cannot be excluded by the observations made in this study, these reactions are not capable of explaining the star−star coupling in Z-RAFT star polymerization of acrylates. This is, because macromonomers that are formed via β-scission from backbiting-derived midchain radicals exhibit the chain length of a single arm at maximum and would thus, when incorporated into a propagating arm, only double

Scheme 3. Proposed Sequence of Reactions Leading to the Formation of Star−Star Couples in Z-RAFT Star Polymerization of Acrylates[a]

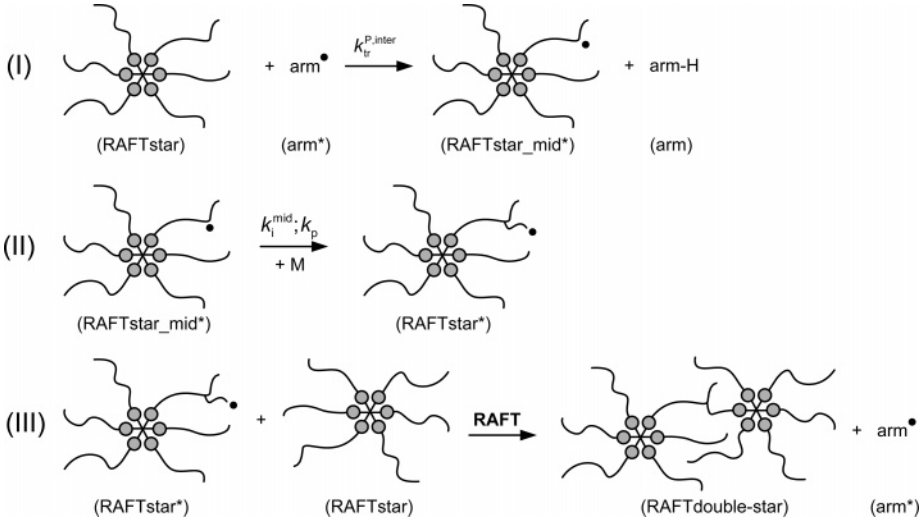

[a] The names in brackets correspond to the species used in the kinetic modeling (see Table 1).

the molecular weight of one individual arm. The resulting overall star polymer would be increased in molecular weight by a factor of 1/6 only. In addition, the mechanism proposed by Postma et al.[36] cannot be harmonized with the occurrence of two cores in the presumed star−star couple.

On the basis of the experimental findings described above and considering the pronounced tendency of polyacrylate macroradicals to undergo transfer to polymer, we propose a sequence of reactions that induce star−star coupling in Z-RAFT star polymerization (see Scheme 3). (I) First, an *inter*molecular transfer to polymer step transfers the radical center from the growing macroradical to a living star polymer, (II) second, the generated midchain radical may reinitiate and propagate to some extent, and (III) third, the propagating radical, which is now located at the star polymer, will finally undergo a RAFT reaction step with other living star polymers resulting in star−star coupling.

Two alternative pathways leading to star−star coupling can be excluded of being significant: First, the coupling of two intermediate RAFT radicals, i.e., so-called self-termination,[51] may also result in a star−star coupling. Termination reactions between two trithiocarbonate-derived intermediate radicals are, however, extremely unlikely, because they constitute a three-arm star with the radical being located in the center. This topology, which in the present star polymerization is additionally located near the center of the overall star polymer, makes the encounter of two such radicals highly unlikely, as is also evident from pair-distribution functions of star-branched chains.[52] In addition, the resulting termination product would continuously be formed from the very beginning of the polymerization and not be generated at elevated monomer conversions only.

Second, the termination between two stars carrying the radical center (see species RAFTstar_mid* and RAFTstar* in Scheme 3) will also induce star−star coupling, similar to the reaction occurring in R-RAFT star polymerization. The contribution of this termination, however, was found by simulations (see below) to be more than 5 orders of magnitude lower than the star−star coupling via the RAFT reaction. This is so, because the star polymer species that carry a radical center (RAFTstar_mid* and RAFTstar*) have extremely low concentrations, as the propagating radical is located on the star polymer for a very short time period only, before it undergoes a RAFT step and becomes a linear arm macroradical again (see Scheme 3). It is thus much more likely for the star polymer radical to react with RAFT agent, which is present in much higher concentrations, than to undergo termination with other star polymer radicals.

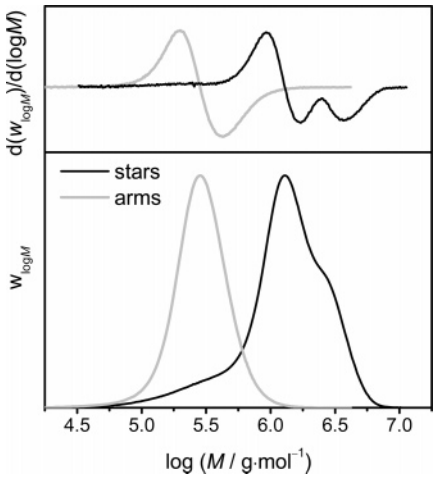

Figure 7. Normalized molecular weight distributions (SEC curves from RI-detection) and first derivatives of star polymer (stars) and of cleaved arms (arms). Star polymer was obtained from **2**-mediated (c_2 = 0.44 × 10^{-3} mol·L^{-1}) AIBN-initiated (c_{AIBN} = 1.71 × 10^{-3} mol·L^{-1}) Z-RAFT star polymerization of BA in bulk at 60 °C after 58% of monomer conversion.

In order to support the mechanism proposed in Scheme 3, which is in harmony with all experimental findings of the present study, we performed star cleavage reactions of star polymer samples obtained after high monomer conversion. Since in Z-RAFT star polymerizations the arms are linked to the core via reactive trithiocarbonate-moieties, star degradation is easily achieved via a single RAFT step using an excess of small initiator-derived radicals.[37,53] Figure 7 depicts the molecular weight distribution of a poly(BA) from Z-RAFT star polymerization mediated by **2**, which exhibits pronounced star−star coupling. The parent star polymer sample shows a trimodal distribution, which is also evident from the first derivative presented in the upper part of the figure. The star polymer features a main peak molecular weight of M_p(star) = 1.30 × 10^6 g·mol^{-1} and a PDI(star) value of 1.93. After cleavage of the star polymer sample, only one monomodal and narrowly distributed polymer species can be observed. It is evident that both the single star as well as the presumed star−star couple

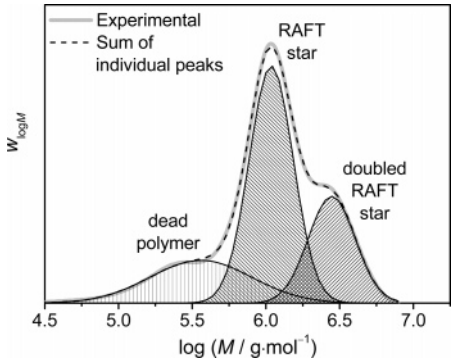

Figure 8. Separation of the molecular weight distribution (SEC curve from RI-detection) of polymer from a **2**-mediated ($c_2 = 0.44 \times 10^{-3}$ mol·L^{-1}) AIBN-initiated ($c_{AIBN} = 1.71 \times 10^{-3}$ mol·L^{-1}) BA bulk RAFT star polymerization at 60 °C after 79.3% of monomer conversion into its individual components via multiple Gaussian peak fitting.

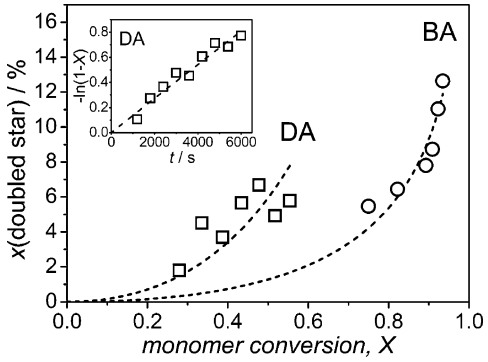

Figure 9. Number fraction, x, of doubled stars vs monomer conversion, X, occurring in (○) **2**-mediated ($c_2 = 0.84 \times 10^{-3}$ mol·L^{-1}) AIBN-initiated ($c_{AIBN} = 5.6 \times 10^{-3}$ mol·L^{-1}) Z-RAFT star polymerization of BA in bulk at 60 °C, and in (□) **2**-mediated ($c_2 = 1.52 \times 10^{-3}$ mol·L^{-1}) AIBN-initiated ($c_{AIBN} = 1.6 \times 10^{-3}$ mol·L^{-1}) Z-RAFT star polymerization of DA in bulk at 60 °C. The inset depicts the pseudo-first-order rate plot of the DA polymerization. The dashed lines are simulations (for details see text).

were fragmented into their individual arms, which exhibit a molecular weight of M_p(arm) $= 0.27 \times 10^6$ g·mol^{-1}. From the molecular weight of the main peak, which is considered to be the single star polymer molecule, and from the molar mass of the arm polymer, it can be concluded that the apparent molecular weights of the star polymer obtained via SEC using linear polymer standards are about 20% smaller than their true values. The low PDI values of the arm polymer, i.e., PDI(arm) = 1.30, indicate that the relatively high polydispersities at elevated monomer conversion in Z-RAFT star polymerization of acrylates is very likely to be due to the star−star coupling effect, but is not due to any loss in molecular weight control. As also evident from the derivative curve, no high molecular weight material can be observed with the arm polymer. Such material would have been expected for mechanisms other than the coupling RAFT step, e.g., coupling via termination or copolymerization of macromonomers, as such reactions would generate a linking polymer between two stars that exhibits a doubled chain length in comparison to the arm polymer.

On the basis of the assumption that the reaction scheme presented in Scheme 3 is correct, it is tempting to evaluate the molecular weight data from Z-RAFT star polymerizations of acrylates quantitatively with respect to the rate coefficient of the *inter*molecular transfer to polymer. This kinetic value will consequently be model dependent. For assessing this parameter, the molecular weight distributions obtained from **2**-mediated BA and DA polymerizations were separated into their individual components via multiple Gaussian peak fitting, as illustrated in Figure 8. When using the RI-detection-derived chain-length distributions, three components could be separated, i.e., the terminated polymer, the star polymer, and the star−star couple. The Gaussian peaks are a first approximation for the true molecular weight distributions, which may, especially in the case of the terminated polymer, exhibit slightly different shapes. The molar concentrations of the individual contributions obtained from the w_{logM} distribution were calculated by usage of their individual number-average molecular weights. This data agreed very well with the results from peak separation of the UV-detection-derived x_{logM} distribution, which directly yielded the necessary molar concentrations data of the individual living components after correction of their respective absorbance strength. The coupling in **2**-mediated MA polymerization was not pronounced enough at monomer conversions of up to 90% to perform meaningful peak separations.

The peak separation yielded the number fraction of star−star couples of the total amount of living polymer as a function of monomer conversion. In a first assumption, every coupled star was considered to be a doubled star, which is in accordance to the findings described above. It is however clear that at further increased monomer conversion the reaction steps proposed in Scheme 3 will also occur with already doubled stars, yielding tripled stars, etc. The occurrence of material with molecular weights that are exceeding double the molar mass of the living star polymer were indeed observed experimentally at very high monomer conversions. The corresponding chain-length distributions, however, are not easily separated into their individual components, which impeded the modeling. Inspection of Figure 9, in which the number fraction of coupled stars in two representative experimental runs of **2**-mediated BA and **2**-mediated DA polymerization are depicted, clearly indicates that the amount of doubled stars is a strong function of monomer conversion, as expected for an effect that originates from transfer to polymer, and that the formation of doubled stars sets in much earlier in DA polymerization. The latter observation is in accordance with studies into concentrations of midchain radicals both in BA and DA polymerization, which suggest that DA exhibits stronger transfer to polymer, both *inter*- and *intra*molecular.[50,54]

In order to arrive at a quantitative parameter that characterizes the intermolecular transfer to polymer in BA and DA polymerization, i.e., the rate coefficient of intermolecular chain transfer to polymer, $k_{tr}^{P,inter}$, the experimental number fraction of doubled stars vs monomer conversion data was modeled via the kinetic simulation program PREDICI. Table 1 gives the employed reaction scheme and the input parameters for the modeling procedure on the example of **2**-mediated BA polymerization at 60 °C. The kinetic modeling was performed in molar concentrations of species only. The average chain length of the star polymer, $\bar{P}_n$(star), was calculated during the simulation from actual monomer conversions via eq 1. In order to implement a correct correlation within the simulation between monomer conversion and time, the experimental monomer conversion vs time traces (i.e., pseudo first-order rate plots) were modeled simultaneously (see inset in Figure 9) via adjustment of the initiator efficiency f. This procedure became necessary, as the literature known kinetic parameters for the respective conventional radical polymerizations were not capable of predicting fully exact monomer conversion vs time curves. This is mainly due to small rate retardation effects,[51] which are frequently observed with RAFT polymerizations, but also due to the occurrence of significant concentrations of midchain radicals, which alter the classical kinetics of radical polymerization (see

Table 1. Reaction Scheme Used for Modeling Star−Star Coupling in the Z-RAFT Star Polymerization of BA at 60 °C in Bulk

	rate coeff	ref
Primary Radical Formation and Initiation[a]		
AIBN → $f \times$ IP* + $f \times$ IP*	$k_d = (1.103 \times 10^{-5}\ s^{-1})$; f	44
IP* + BA → arm*	$k_i = 1.3 \times 10^3\ L{\cdot}mol^{-1}{\cdot}s^{-1}$	57
Propagation		
arm* + BA → arm*	$k_p = 3.5 \times 10^4\ L{\cdot}mol^{-1}{\cdot}s^{-1}$	58
RAFTstar* + BA → RAFTstar*	$k_p = 3.5 \times 10^4\ L{\cdot}mol^{-1}{\cdot}s^{-1}$	58
Termination		
arm* + arm* → polyBA	$k_t = 6.0 \times 10^7\ L{\cdot}mol^{-1}{\cdot}s^{-1}$ [b]	55
Transfer to Polymer (Intermolecular)		
arm* + RAFTstar → RAFTstar_mid* + polyBA	$\bar{P}_n$(star) $\times\ k_{tr}^{P,inter}$ [c]	
Reinitiation of the Midchain Radical		
RAFTstar_mid* + BA → RAFTstar*	$k_{i\_mid} = 67\ L{\cdot}mol^{-1}{\cdot}s^{-1}$ [c]	59
Star−Star Coupling by a RAFT Step		
RAFTstar* + RAFTstar → RAFTdouble-star + arm*	$k_{ex} =$ NTT $\times\ 1.5 \times 10^6\ L{\cdot}mol^{-1}{\cdot}s^{-1}$ [d]	60
Termination of Star Polymer		
RAFTstar* + arm* → RAFTstar	$k_t = 6.0 \times 10^7\ L{\cdot}mol^{-1}{\cdot}s^{-1}$ [b]	55
RAFTstar* + RAFTstar* → RAFTdouble−star	$k_t = 6.0 \times 10^7\ L{\cdot}mol^{-1}{\cdot}s^{-1}$ [b]	55
RAFTstar_mid* + arm* → RAFTstar	$k_{t\_mid} = 2.0 \times 10^7\ L{\cdot}mol^{-1}{\cdot}s^{-1}$ [b,e]	59
RAFTstar_mid* + RAFTstar* → RAFTdouble−star	$k_{t\_mid} = 2.0 \times 10^7\ L{\cdot}mol^{-1}{\cdot}s^{-1}$ [b,e]	59
RAFTstar_mid* + RAFTstar_mid* → RAFTdouble−star	$k_{t\_mid\_mid} = 1.4 \times 10^6\ L{\cdot}mol^{-1}{\cdot}s^{-1}$ [b,e]	59

[a] IP* = 2-cyano-isopropyl radical; for other species see Scheme 3. [b] Termination rate coefficients are given for the IUPAC recommended rate laws $R_{term} = -2k_t c_R^2$. [c] $\bar{P}_n$(star) denotes the number-average chain-length of star polymer. [d] NTT indicates the number of active RAFT-agent moieties per star molecule (NTT = 6 in this work). [e] Values were reported for 50 °C.

below).[55] The rate of intermolecular transfer to polymer was implemented into the simulation as being proportional to the average chain length of the attacked star polymer, $\bar{P}_n$(star), which is commonly used in simulating transfer to polymer.[56] The evaluated $k_{tr}^{P,inter}$ values thus denote the rate coefficient of intermolecular chain transfer to a polymer repeat unit. In the kinetic modeling procedure two parameters, i.e., f and $k_{tr}^{P,inter}$, were simultaneously fitted to two individual experimental data sets, i.e., time-dependent monomer conversion and number fraction of doubled stars. The resulting parameters can hence be considered of high statistic significance.

It should be noted that *intra*molecular chain transfer (backbiting) will also readily occur in all of the studied acrylate polymerizations. As this reaction step is not reflected in any of the investigated polymer characteristics, it was not implemented in the modeling. This approximation may lead to calculated concentrations of propagating radicals that are slightly incorrect, as the kinetics of radical polymerization is changed when substantial amounts of midchain radicals occur.[55] The internal correlation between monomer conversion and time, for which purpose the propagating radical concentration was modeled via the adjustment of f, remains, however, correct. The estimated $k_{tr}^{P,inter}$ values are also not affected by uncertainties in the propagating radical concentration (see below).

The implemented reaction scheme was capable of modeling the experimental evolution of star−star coupling with monomer conversion with surprisingly good agreement (see Figure 9), lending credit to the plausibility of the proposed reaction mechanism. The best fit results obtained for individual experimental runs of BA polymerization are presented in Table 2. The average value for the rate coefficient of intermolecular transfer to polymer in butyl acrylate polymerization at 60 °C is

$$k_{tr}^{P,inter}\ (BA, 60\ °C) = 0.33 \pm 0.11\ L{\cdot}mol^{-1}{\cdot}s^{-1}$$

with the error being the standard deviation.

As mentioned above, the simulated amount of star−star couples that originate from termination between star polymer species that carry a radical center, i.e., from termination of various combinations of RAFTstar_mid* and RAFTstar*, was

Table 2. Modeling Results of Individual Experimental Runs for the Rate Coefficient of Intermolecular Chain Transfer to a Polymer Repeat Unit, $k_{tr}^{P,inter}$, in 2-Mediated BA Bulk Polymerization at 60 °C

run no.	c_2/mol·L^{-1}	c_{AIBN}/mol·L^{-1}	$k_{tr}^{P,inter}$/L·mol^{-1}·s^{-1}
1	0.84×10^{-3}	1.83×10^{-3}	0.23
2	0.44×10^{-3}	1.71×10^{-3}	0.49
3	0.83×10^{-3}	3.70×10^{-3}	0.29
4	0.84×10^{-3}	5.60×10^{-3}	0.30

Table 3. Modeling Results of Individual Experimental Runs for the Rate Coefficient of Intermolecular Chain Transfer to a Polymer Repeat Unit, $k_{tr}^{P,inter}$, in 2-Mediated DA Bulk Polymerization at 60 °C[a]

run no.	c_2/mol·L^{-1}	c_{AIBN}/mol·L^{-1}	$k_{tr}^{P,inter}$/L·mol^{-1}·s^{-1}
1	1.52×10^{-3}	1.55×10^{-3}	6.0
2	3.29×10^{-3}	1.77×10^{-3}	8.2

[a] Kinetic parameters used in the modeling: $k_i = 1.3 \times 10^3\ L{\cdot}mol^{-1}{\cdot}s^{-1}$;[57] $k_p = 38\,500\ L{\cdot}mol^{-1}{\cdot}s^{-1}$;[61] $k_t = 1.0 \times 10^7\ L{\cdot}mol^{-1}{\cdot}s^{-1}$;[61] $k_{ex} = 2.4 \times 10^6\ L{\cdot}mol^{-1}{\cdot}s^{-1}$; [62] $k_{i\_mid} = 73\ L{\cdot}mol^{-1}{\cdot}s^{-1}$

2×10^5 times smaller than the amount of stars from the RAFT reaction in the case of the BA system. Thus, star−star coupling by radical−radical termination was ignored when modeling the DA system, for which the corresponding reaction coefficients k_{t_mid} and $k_{t\_mid\_mid}$ are not exactly known. The reinitiation rate coefficient of the midchain radical, k_{i_mid}, for the DA system was assumed larger than k_{i_mid} for the BA system by the same factor as the propagation rate coefficient. The best fit results obtained for two DA polymerizations are presented in Table 3. The modeling of all experimental runs was not possible, as using low RAFT agent concentrations resulted in broad chain-length distributions (see PDI values in Figure 3), which impeded the peak separation. The average value for the rate coefficient of intermolecular transfer to polymer in dodecyl acrylate polymerization at 60 °C is

$$k_{tr}^{P,inter}\ (DA, 60\ °C) = 7.1 \pm 1.6\ L{\cdot}mol^{-1}{\cdot}s^{-1}$$

with the error being the standard deviation.

Intermolecular chain transfer to polymer was found to be more than ten times faster in DA polymerization than in the

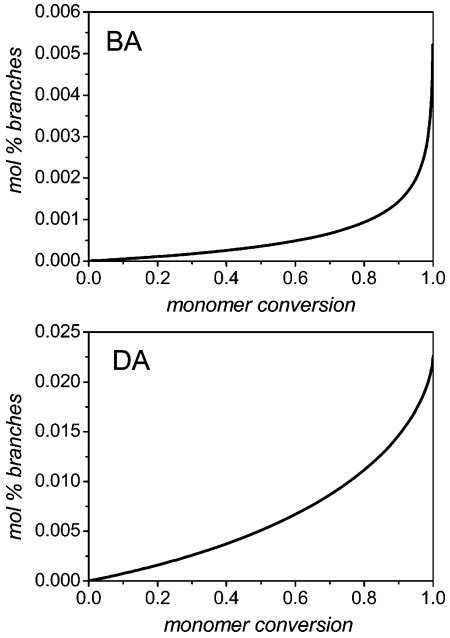

Figure 10. Simulated mole percent of long-chain branches in poly(butyl acrylate) and poly(dodecyl acrylate) prepared by radical polymerization of BA and DA, respectively, at 60 °C.

BA system. This result is in agreement with studies into midchain radical concentrations, which where determined to be higher in the DA system than with BA radical polymerization.[50,54] Although most of the midchain radicals in acrylate polymerization are formed via backbiting, the overall concentration of midchain radicals is assumed to be an indication for the ability of the respective macroradicals to abstract hydrogen from the polymer chain. The MA system apparently exhibits the smallest hydrogen abstraction frequency of the studied systems, evidenced by the small extent of star−star coupling.

There is little data in the literature to which the estimated $k_{tr}^{P,inter}$ values can be compared. Arzamandi et al.[56] reported a $k_{tr}^{P,inter}$ value for the ethyl acrylate polymerization at 60 °C of 0.01 $L \cdot mol^{-1} \cdot s^{-1}$, based on the modeling of conventional emulsion polymerization. This value is by 1 order of magnitude smaller than the value found for BA, which is in qualitative agreement with the scenario found in this study that the rate of transfer to polymer is slower with acrylates having smaller ester-moieties.

By using the reaction mechanism given in Table 1 and the rate coefficients for transfer to polymer reported above, the extent of branching as a function of monomer conversion can be calculated. Figure 10 depicts the mole percent of long-chain branches as a function of monomer conversion occurring in polyBA and polyDA prepared by radical polymerization at 60 °C. It is important to note that the mole percent of long-chain branches is independent of both the radical flux during the polymerization process and the initial monomer concentration, when using the basic reaction scheme given in Table 1. The latter has been confirmed experimentally in BA solution polymerization with initial monomer concentrations above 10 wt %.[63] The effects of chain-length and monomer conversion on various kinetic parameters have not been accounted for in the presented simulation, which may complicate the situation.

Comparison of the mole percent of long-chain branches in the BA system (see Figure 10) with the total fraction of branched repetitive monomer units, which has been determined by Ahmad et al. to be around 2% in polyBA generated at 70 °C,[63] indicates that the vast amount of branches in polyBA results from *intra*molecular chain transfer to polymer (backbiting). This finding is in line with the study by Farcet et al.,[64] who arrived at the same conclusion after performing end group determination of polyBA generated via nitroxide-mediated polymerization.

The method presented here, which is based on the evaluation of Z-RAFT star polymerizations, is in principle capable of determining *inter*molecular transfer to polymer events separately from *intra*molecular transfer to polymer. Commonly, the transfer to polymer rate coefficients are evaluated from the total amount of branches, which gives information about the overall extent of transfer to polymer. However, determining long-chain branching originating from *inter*molecular transfer to polymer next to short-chain branches generated via *intra*molecular transfer to polymer (backbiting) is not trivial with conventional methods.[63] The employment of Z-RAFT star polymerization, however, provides a unique pathway for easily separating short-chain from long-chain branching and may hence become a useful tool for studies into the transfer to polymer reaction.

From the viewpoint of an experimentalist who desires the formation of uniform star polymer via Z-RAFT star polymerization, the following conclusions from simulations using the mechanistic scheme given in Table 1 are important: (i) In order to minimize star−star coupling, the mass fraction of polymer in the system has to be kept as low as possible. This can either be achieved by stopping the polymerization at relatively low monomer conversion or by performing the polymerizations in solution. Both approaches, however, result in reduced maximum molecular weights. In addition, RAFT polymerizations performed in solution are sometimes beset with inferior molecular weight control. (ii) The molar fraction of star−star couples can also be reduced by increasing the RAFT agent concentration, whereby the constant number of branches (see Figure 10) is distributed among an increased amount of star polymer molecules. However, such an approach also reduces the maximum accessible chain length. (iii) The effect of star−star coupling occurring at higher monomer conversion can in principle not be avoided by reducing the initiator concentration.

In the case the activation energy and activation volume of the $k_{tr}^{P,inter}$ value are significantly different from the activation parameters of propagation, variation in temperature and pressure may impact the extent of star−star coupling. These studies are currently underway in our laboratory in order to further optimize the Z-RAFT star polymerization of acrylates.

Conclusions

Z-RAFT star polymerizations using a hexafunctional trithiocarbonate, in which the mediating RAFT-agent moieties are interlinked to the core molecule via the stabilizing Z-group, provide access to well-defined star polymers of methyl acrylate, butyl acrylate, and dodecyl acrylate with predictable molecular weights up to more than 1 million $g \cdot mol^{-1}$ in some cases. Narrow molecular weight distributions with PDI values well below 1.5 are obtained up to intermediate monomer conversions and molecular weights of several hundreds of thousand $g \cdot mol^{-1}$.

At intermediate and high monomer conversions, the unexpected occurrence of high molecular weight components induces broadening of the molecular weight distributions of the generated star polymer. This effect increases significantly when going from MA to BA and DA polymerization. The high molecular weight material was demonstrated to result from star−star coupling reactions, which most likely arise from *inter*molecular transfer to polymer. The living RAFT process itself, however, was found to be very effective up to high monomer conversions, as evidenced from star polymer cleavage reactions. This finding

indicates that steric congestion near the core of the star polymer molecule does not hamper the RAFT equilibrium significantly in the Z-RAFT star polymerization of acrylate.

The amount of star−star couples, which is a direct measure for the extent of long-chain branching, was quantified as a function of monomer conversion and subsequently modeled via computer simulations. By this approach, the rate coefficient of *inter*molecular transfer to polymer could be estimated for BA and DA radical polymerization and was found to be more than 1 order of magnitude higher in the DA system than in BA polymerization.

Acknowledgment. Financial support granted by the Deutsche Forschungsgemeinschaft for project VA226/3-1 and within the frame of the European Graduate School "Microstructural Control in Free-Radical Polymerization" is gratefully acknowledged. The authors thank Prof. Michael Buback (University of Göttingen) for continuous support.

References and Notes

(1) McLeish, T. C. B.; Milner, S. T. Entangled dynamics and melt flow of branched polymers. In *Branched Polymers II*; Roovers, J., Ed.; Springer: Heidelberg, 1999; Vol. 143, pp 195−256.
(2) Gabriel, C.; Munstedt, H. *Rheol. Acta* **2002**, *41*, 232−244.
(3) Lee, J. H.; Goldberg, J. M.; Fetters, L. J.; Archer, L. A. *Macromolecules* **2006**, *39*, 6677−6685.
(4) McLeish, T. C. B. *Chem. Eng. Res. Des.* **2000**, *78*, 12−32.
(5) Hadjichristidis, N.; Pispas, S.; Pitsikalis, M.; Iatrou, H.; Vlahos, C. Asymmetric star polymers: Synthesis and properties. In *Branched Polymers I*; Roovers, J., Ed.; Springer: Heidelberg, 1999; Vol. 142, pp 71−127.
(6) Claesson, H.; Malmstrom, E.; Johansson, M.; Hult, A. *Polymer* **2002**, *43*, 3511−3518.
(7) Stenzel-Rosenbaum, M. H.; Davis, T. P.; Fane, A. G.; Chen, V. *Angew. Chem., Int. Ed.* **2001**, *40*, 3428−3432.
(8) Barner-Kowollik, C.; Davis, T. P.; Heuts, J. P. A.; Stenzel, M. H.; Vana, P.; Whittaker, M. *J. Polym. Sci., Part A: Polym. Chem.* **2003**, *41*, 365−375.
(9) Qiu, L. Y.; Bae, Y. H. *Pharm. Res.* **2006**, *23*, 1−30.
(10) Jones, M. C.; Ranger, M.; Leroux, J. C. *Bioconjugate Chem.* **2003**, *14*, 774−781.
(11) Jie, P.; Venkatraman, S. S.; Min, F.; Freddy, B. Y. C.; Huat, G. L. *J. Controlled Release* **2005**, *110*, 20−33.
(12) Matyjaszewski, K.; Davis, T. P. *Handbook of radical polymerization.* Wiley-Interscience: Hoboken, NJ, 2002.
(13) Taton, D.; Gnanou, Y.; Matmour, R.; Angot, S.; Hou, S.; Francis, R.; Lepoittevin, B.; Moinard, D.; Babin, J. *Polym. Int.* **2006**, *55*, 1138−1145.
(14) Pitto, V.; Voit, B. I.; Loontjens, T. J. A.; van Benthem, R. *Macromol. Chem. Phys.* **2004**, *205*, 2346−2355.
(15) Lecolley, F.; Waterson, C.; Carmichael, A. J.; Mantovani, G.; Harrisson, S.; Chappell, H.; Limer, A.; Williams, P.; Ohno, K.; Haddleton, D. M. *J. Mater. Chem.* **2003**, *13*, 2689−2695.
(16) Matyjaszewski, K. *Polym. Int.* **2003**, *52*, 1559−1565.
(17) Matyjaszewski, K.; Miller, P. J.; Pyun, J.; Kickelbick, G.; Diamanti, S. *Macromolecules* **1999**, *32*, 6526−6535.
(18) Xue, L.; Agarwal, U. S.; Zhang, M.; Staal, B. B. P.; Muller, A. H. E.; Bailly, C. M. E.; Lemstra, P. J. *Macromolecules* **2005**, *38*, 2093−2100.
(19) Matyjaszewski, K.; Xia, J. *Chem. Rev.* **2001**, *101*, 2921−2990.
(20) Hawker, C. J.; Bosman, A. W.; Harth, E. *Chem. Rev.* **2001**, *101*, 3661−3688.
(21) Moad, G.; Rizzardo, E.; Thang, S. H. *Aust. J. Chem.* **2005**, *58*, 379−410.
(22) Stenzel-Rosenbaum, M.; Davis, T. P.; Chen, V.; Fane, A. G. *J. Polym. Sci., Part A: Polym. Chem.* **2001**, *39*, 2777−2783.
(23) Boschmann, D.; Vana, P. *Polym. Bull. (Heidelberg, Ger.)* **2005**, *53*, 231−242.
(24) Chen, M.; Ghiggino, K. P.; Launikonis, A.; Mau, A. W. H.; Rizzardo, E.; Sasse, W. H. F.; Thang, S. H.; Wilson, G. J. *J. Mater. Chem.* **2003**, *13*, 2696−2700.
(25) Mayadunne, R. T. A.; Jeffery, J.; Moad, G.; Rizzardo, E. *Macromolecules* **2003**, *36*, 1505−1513.
(26) Darcos, V.; Dureault, A.; Taton, D.; Gnanou, Y.; Marchand, P.; Caminade, A. M.; Majoral, J. P.; Destarac, M.; Leising, F. *Chem. Commun.* **2004**, 2110−2111.
(27) Bernard, J.; Favier, A.; Zhang, L.; Nilasaroya, A.; Davis, T. P.; Barner-Kowollik, C.; Stenzel, M. H. *Macromolecules* **2005**, *38*, 5475−5484.
(28) Zhang, L. W.; Chen, Y. M. *Polymer* **2006**, *47*, 5259−5266.
(29) Stenzel, M. H.; Davis, T. P. *J. Polym. Sci., Part A: Polym. Chem.* **2002**, *40*, 4498−4512.
(30) Pyun, J.; Rees, I.; Frechet, J. M. J.; Hawker, C. J. *Aust. J. Chem.* **2003**, *56*, 775−782.
(31) Huang, C. F.; Lee, H. F.; Kuo, S. W.; Xu, H. Y.; Chang, F. C. *Polymer* **2004**, *45*, 2261−2269.
(32) Chaffey-Millar, H.; Stenzel, M. H.; Davis, T. P.; Coote, M. L.; Barner-Kowollik, C. *Macromolecules* **2006**, *39*, 6406−6419.
(33) Jesberger, M.; Barner, L.; Stenzel, M. H.; Malmstrom, E.; Davis, T. P.; Barner-Kowollik, C. *J. Polym. Sci., Part A: Polym. Chem.* **2003**, *41*, 3847−3861.
(34) Moad, G.; Mayadunne, R. T. A.; Rizzardo, E.; Skidmore, M.; Thang, S. H. *ACS Symp. Ser.* **2003**, *854*, 520−535.
(35) Davis, K. A.; Paik, H. J.; Matyjaszewski, K. *Macromolecules* **1999**, *32*, 1767−1776.
(36) Postma, A.; Davis, T. P.; Li, G. X.; Moad, G.; O'Shea, M. S. *Macromolecules* **2006**, *39*, 5307−5318.
(37) Perrier, S.; Takolpuckdee, P.; Mars, C. A. *Macromolecules* **2005**, *38*, 6770−6774.
(38) Strazielle, C.; Benoit, H.; Vogl, O. *Eur. Polym. J.* **1978**, *14*, 331−334.
(39) Buback, M.; Feldermann, A.; Barner-Kowollik, C.; Lacik, I. *Macromolecules* **2001**, *34*, 5439−5448.
(40) Beuermann, S.; Paquet, D. A.; McMinn, J. H.; Hutchinson, R. A. *Macromolecules* **1996**, *29*, 4206−4215.
(41) Buback, M.; Kurz, C. H.; Schmaltz, C. *Macromol. Chem. Phys.* **1998**, *199*, 1721−1727.
(42) Buback, M.; Frauendorf, H.; Vana, P. *J. Polym. Sci., Part A: Polym. Chem.* **2004**, *42*, 4266−4275.
(43) Vana, P.; Davis, T. P.; Barner-Kowollik, C. *Aust. J. Chem.* **2002**, *55*, 315−318.
(44) Grulke, E. A.; Brandrup, J.; Immergut, E. H. *Polymer Handbook.* 4th ed.; Wiley-Interscience: New York and Chichester, U.K., 1999.
(45) Buback, M.; Huckestein, B.; Kuchta, F. D.; Russell, G. T.; Schmid, E. *Macromol. Chem. Phys.* **1994**, *195*, 2117−2140.
(46) Charton, N.; Feldermann, A.; Theis, A.; Stenzel, M. H.; Davis, T. P.; Barner-Kowollik, C. *J. Polym. Sci., Part A: Polym. Chem.* **2004**, *42*, 5170−5179.
(47) Sun, T.; Chance, R. R.; Graessley, W. W.; Lohse, D. J. *Macromolecules* **2004**, *37*, 4304−4312.
(48) Buback, M.; Junkers, T.; Vana, P. *Macromol. Rapid Commun.* **2005**, *26*, 796−802.
(49) Hutchinson, R. A.; Aronson, M. T.; Richards, J. R. *Macromolecules* **1993**, *26*, 6410−6415.
(50) Willemse, R. X. E.; van Herk, A. M.; Panchenko, E.; Junkers, T.; Buback, M. *Macromolecules* **2005**, *38*, 5098−5103.
(51) Barner-Kowollik, C.; Buback, M.; Charleux, B.; Coote, M. L.; Drache, M.; Fukuda, T.; Goto, A.; Klumperman, B.; Lowe, A. B.; Mcleary, J. B.; Moad, G.; Monteiro, M. J.; Sanderson, R. D.; Tonge, M. P.; Vana, P. *J. Polym. Sci., Part A: Polym. Chem.* **2006**, *44*, 5809−5831.
(52) Zifferer, G. *Macromol. Theory Simul.* **2000**, *9*, 479−487.
(53) Nguyen, D. H.; Vana, P. *Polym. Adv. Technol.* **2006**, *17*, 625−633.
(54) Müller, E. Detailed Investigations into the Propagation and Termination Kinetics of Bulk Homo- and Copolymerization of (Meth)Acrylates. Ph.D. Thesis, University of Göttingen, Göttingen, Germany, 2005.
(55) Junkers, T.; Theis, A.; Buback, M.; Davis, T. P.; Stenzel, M. H.; Vana, P.; Barner-Kowollik, C. *Macromolecules* **2005**, *38*, 9497−9508.
(56) Arzamendi, G.; Forcada, J.; Asua, J. M. *Macromolecules* **1994**, *27*, 6068−6079.
(57) Fischer, H.; Radom, L. *Angew. Chem., Int. Ed.* **2001**, *40*, 1340−1371.
(58) Asua, J. M.; Beuermann, S.; Buback, M.; Castignolles, P.; Charleux, B.; Gilbert, R. G.; Hutchinson, R. A.; Leiza, J. R.; Nikitin, A. N.; Vairon, J. P.; van Herk, A. M. *Macromol. Chem. Phys.* **2004**, *205*, 2151−2160.
(59) Nikitin, A. N.; Hutchinson, R. A. *Macromol. Theory Simul.* **2006**, *15*, 128−136.
(60) Buback, M.; Hesse, P.; Junkers, T.; Vana, P. *Macromol. Rapid Commun.* **2006**, *27*, 182−187.
(61) Beuermann, S.; Buback, M. *Prog. Polym. Sci.* **2002**, *27*, 191−254.
(62) Theis, A.; Feldermann, A.; Charton, N.; Davis, T. P.; Stenzel, M. H.; Barner-Kowollik, C. *Polymer* **2005**, *46*, 6797−6809.
(63) Ahmad, N. M.; Heatley, F.; Lovell, P. A. *Macromolecules* **1998**, *31*, 2822−2827.
(64) Farcet, C.; Belleney, J.; Charleux, B.; Pirri, R. *Macromolecules* **2002**, *35*, 4912−4918.

MA0627626